

Valence of D_{5h} C_{50} FullereneZijian Xu,^{*,†,‡} Jianguang Han,^{†,‡} Zhiyuan Zhu,[†] and Wei Zhang[§]

Shanghai Institute of Applied Physics, Chinese Academy of Sciences, Shanghai 201800, People's Republic of China, Graduate School of Chinese Academy of Sciences, Beijing 100049, People's Republic of China, and The Key Laboratory of Beam Technology and Material Modification of Ministry of Education, Institute of Low Energy Nuclear Physics, Beijing Normal University, Beijing 100875, People's Republic of China

Received: July 16, 2006; In Final Form: November 11, 2006

The energetic and electronic properties of D_{5h} C_{50} before and after passivation by H or Cl are investigated using first-principle computational method of density functional theory with generalized gradient approximation and local density approximation functionals. The results show that H or Cl addition can lead to energetic stabilization. Additions also increase the highest occupied molecular orbit–lowest unoccupied molecular orbital (HOMO–LUMO) gaps of C_{50} fullerenes and make them chemically more stable. In the series of $C_{50}H_{2m}$ ($m = 0\sim 7$), the Saturn-shaped D_{5h} $C_{50}H_{10}$ has the largest HOMO–LUMO gap, which suggests that such a structure of $C_{50}H_{10}$ is a “magic-number” stable one of C_{50} adducts, and ten is a pseudovalence or effective valence of C_{50} fullerene pseudoatom. This point also is supported by the energetic properties of $C_{50}H_{2m}$ series such as binding energies, etc. A minimal energy reaction pathway is constructed to get $C_{50}H_{10}$ and $C_{50}H_{14}$. Some useful experience for determining the favorable addition sites was summarized. A simple steric method is developed to predict the effective valences of classical fullerenes.

Introduction

Since the discovery of C_{60} in 1985,¹ caged forms of carbon clusters have sparked tremendous scientific interest all over the world because of their novel physical and chemical properties. Most work until now has been focused on C_{60} and its larger homologs, which faithfully satisfy the isolated pentagon rule (IPR).^{2,3} The smaller non-IPR fullerenes (C_n with $n < 60$) are of particular interest because of their high curvature and increased strain energy with adjacent pentagonal rings that greatly decrease the stability of fullerenes^{3–8} but may lead to various adducts,^{6,9–13} oligomers,^{7,12,14,15} polymers,^{12,16} and solids^{5,12,14,17} with unusual bonding and electronic properties. Piskoti et al.⁵ synthesized C_{36} crystal by the arc-discharge method, which is the first time that a fullerene smaller than C_{60} has been produced massively. Xie et al.¹⁸ first synthesized $C_{50}Cl_{10}$ in macroscopic scale with the purity of 99.5%. According to ¹³C NMR measurement, they inferred that this molecule has a Saturn-shaped structure of D_{5h} symmetry as shown in Figure 1b in which 10 Cl atoms are added to 10 equatorial carbons of C_{50} . These C sites are believed to be the most active sites in C_{50} because they are vertex fusions of two pentagons and one hexagon, and other C sites are just the vertexes of one pentagon and two hexagons. It is generally believed that pentagon adjacencies would decrease the stability of fullerenes.^{3,4,13}

This experimental progress stimulated the theoretical researchers' passion on C_{50} fullerene. In the subsequent theoretical works, the stability and reactivity of C_{50} and its isomers,^{35,36} the addition features and principles,^{34,35,38} the oligomers of D_{5h} C_{50} ,^{34,35} and the excitation spectra of $C_{50}Cl_{10}$ ³⁹ are investigated detailedly. It has been found that the most stable isomer of C_{50} is not D_{5h} C_{50} with 5 pentagon adjacencies but D_3 C_{50} with 6

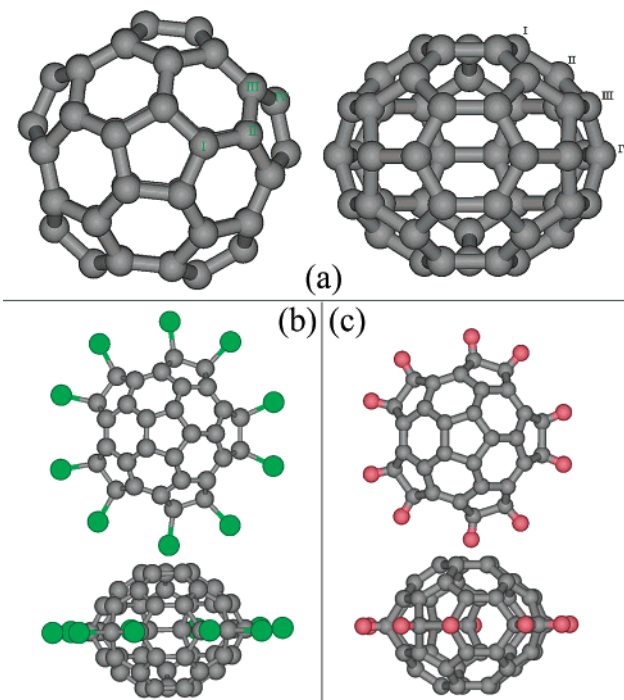


Figure 1. (a) Optimized structure of D_{5h} C_{50} . I, II, III, and IV denote four nonequivalent C sites in this molecule. The left is the top view, the right is the side view. (b) Optimized structure of $C_{50}Cl_{10}$ in which all Cl atoms (green balls) are added to C4 sites. (c) Optimized structure of $C_{50}H_{10}$ in which all H atoms (red balls) are added to type-IV sites.

pentagon adjacencies, which violates the rule of minimum pentagon adjacencies.^{34,35} The ground state of D_{5h} C_{50} has been proven to be singlet state without diradical character.³⁵ Its high reactivity comes from the highly strained equatorial sites of pentagon–pentagon fusions. Structure strain makes the π orbital of these sites stretch out very much and that leads to pyra-

* Corresponding author. E-mail: xuzijian@sinap.ac.cn.

† Shanghai Institute of Applied Physics.

‡ Graduate School of Chinese Academy of Sciences.

§ Beijing Normal University.

midization of the bonding structure of C4 sites and makes the π system become dangling bonds. But why the preferential number of addition atoms is 10 and not 8 or 12 has not been clearly testified by theoretical computation.

Researchers of cluster physics and chemistry have used shell-closing and cluster valence models to study reactivity and stability of clusters.^{9,11,19} It is expected that clusters will fall into places in a generalized periodic table when they are treated as superatoms. Kroto and Walton argued that small fullerene cages might behave as “pseudoatoms” with reactivity patterns determined by maximal aromaticity and minimal steric strain.¹⁹ Each lower fullerene then would have its own characteristic “pseudo-valency”. Milani et al.⁹ suggested that any given fullerene might display additional “hidden” valencies and presented evidence from calculated HOMO–LUMO gaps of some hydrogen-passivated cages. According to this model theory for clusters, such a structure of $C_{50}Cl_{10}$ probably is a characteristic or magic-number pseudo-valency structure of C_{50} fullerene derivatives. From the previous calculations on C_{36} and C_{24} additions,^{10,11} we know that hydrogenated and fluorinated fullerenes have parallel energetic and structural properties, and a valence is a characteristic of the cage but not the addend. Therefore, H, F, or Cl addition should lead to the same predicted valence and $C_{50}H_{10}$ of the same structure as $C_{50}Cl_{10}$ is also a magic-number stable adduct with effective valence equal to 10.

In this paper, we focus on the valence of D_{5h} C_{50} with H additions. A series of molecules $C_{50}H_m$ with $m = 0, 1, 2, 4, 6, 8, 10, 11, 12,$ and 14 have been considered in the study. Structural optimizations and energetic and electronic structure calculations were performed to investigate in detail the stability variation of C_{50} hydrides with m , using first-principle computational method of density functional theory (DFT)²⁰ with generalized gradient approximation (GGA) functional and local density approximation (LDA) functional. We try to prove that 10 is the pseudovalence of D_{5h} C_{50} pseudoatom and the Saturn-shaped $C_{50}H_{10}$ as well as $C_{50}Cl_{10}$ has the magic-number stability in the best isomer series of $C_{50}H_{2m}$. Some cases of C_{50} passivation with Cl atoms have also been studied by the same DFT method and compared with H passivation cases.

Computational Details

All calculations in this paper were performed by use of DFT code FHI98MD.²¹ This code implemented DFT of KS scheme²² by pseudopotential plane-wave method.²³ In our calculations, norm-conserving nonlocal pseudopotentials for C, H, and Cl were generated using FHI98PP code²⁴ and the scheme of Hamann.²⁵ The nonlocal parts of the pseudopotentials were represented using the Kleinman–Bylander fully separable form.²⁶ The PW91 parametrization²⁷ was used for the GGA exchange-correlation functional, and CA/PZ scheme^{28,29} was used for the LDA functional. The PW91 functional has been used successfully to calculate the hydrogenation effect of C_{60} by Yi et al.³⁰ The plane-wave energy cutoff was taken as 40 Ry, which converges the total energy to within 0.1 eV. Such a cutoff energy may be not high enough to converge the total energy to an often adopted high accuracy, such as 1 meV, but convergence errors tend to cancel out when total energy differences are computed.³¹ The shape of supercell is orthorhombic and the box size for $C_{50}H_{10}$ is taken as $28 \times 28 \times 20$ Bohr.³ The boxes for the other molecules are no smaller than that for $C_{50}H_{10}$, and they are all large enough to neglect the effects due to interactions between images. The damped Newton dynamics method was used to optimize the structures of passivated fullerenes without symmetry constraints. The con-

TABLE 1: Isomer Numbers Taken in Our Computations for Each m in $C_{50}H_m$ and $C_{50}Cl_m$

m	$C_{50}H_m$			$C_{50}Cl_m$	
	only site-IV addition	one non-IV addition ^a	two non-IV addition ^b	only site-IV addition	one non-IV addition ^a
1	1	3	0	1	3
2	7	7	33	7	0
4	27	0	0	0	0
6	27	0	0	0	0
8	7	20	119	0	0
10	1	20	124	1	0
11	3			0	
12	42			0	
14	208			0	

^a One non-IV addition means only one atom (H or Cl) is added to nonequatorial site. ^b Two non-IV addition means two atoms are added to non-equatorial sites.

vergence criterion for structural optimization was that the force on each ion is smaller than 0.001 au. Gamma point electronic structure calculations were performed after optimization.

In our DFT computations, electronic structures are treated as closed-shell singlet configurations, which are expected to be the ground states under full geometric relaxation.¹² It has been proven that the ground state of D_{5h} C_{50} is a closed-shell singlet state.³⁵ Hence, the use of the closed-shell DFT scheme is feasible for calculations on C_{50} . Despite this, there may still be some isomers with odd components in our computations. According to simple Hückel theory, they might be radicals and have open-shell configurations.¹¹ However, many of these odd-component structures can achieve a closed-shell ground state by a weak second-order Jahn–Teller distortion in a full optimization.^{11,13,6} Usually, open-shell states are competitive with the closed-shell singlet, and they are close to each other in energy. The difference between the open-shell and the closed-shell state for D_{6h} C_{36} is only about 0.16 eV.^{6,8,32} In addition, there may be some “accidental” radicals that have even components but open-shell ground states. These radicals usually do not affect the closed-shell results because their energies are generally high. According to ref 11, removal of intrinsic radicals can strongly reduce the computational effort but will not change the chemical conclusions. Therefore, using a closed-shell DFT scheme to simulate the isomers of $C_{50}H_{2m}$ is reasonable and feasible.

In our computations on C_{50} addition, m is equal to 1, 2, and 10 for $C_{50}Cl_m$ molecules and is equal to 0, 1, 2, 4, 6, 8, 10, 11, 12, and 14 for $C_{50}H_m$. Obviously, for each m there can be a lot of isomers and everyone of them should be optimized to seek the most stable ones. This will be a prohibitively time-consuming task when it is done by ab initio method. To decrease the number of isomers to be simulated, symmetrical equivalence, empirical rules, and experience derived from computations with smaller m values are used to determine the favorable addition sites. One useful empirical rule from Fowler et al.¹³ is that the addition to a fullerene will give the energy lowering in the order PPP > PPH > PHH > HHH in which the symbols denote the addition sites at which the set of three rings fused, H denotes hexagon, and P denotes pentagon.

On the basis of the above considerations and the fact that all equatorial sites of C_{50} are PPHs while other sites are all PHH ones, we determined the numbers of isomers to be simulated as listed in Table 1. All the chosen isomers are optimized using PW91 functional first. Then, for each m , the most stable 7 or 10 isomers are optimized again using LDA functional. LDA results are compared with GGA results to further verify the conclusions. We mainly adopted the results from the PW91 calculations.

TABLE 2: Bond Lengths^a of Optimized C₅₀ and Its Derivatives Using LDA and GGA Functional

bond type	LDA			GGA			
	C ₅₀	C ₅₀ H ₁₀	C ₅₀ Cl ₁₀	C ₅₀	C ₅₀ H ₁₀	C ₅₀ Cl ₁₀	C ₅₀ Cl ₁₀ ^b
C1–C1	1.440	1.425	1.423	1.450	1.432	1.430	1.438
C1–C2	1.385	1.395	1.395	1.399	1.403	1.403	1.408
C2–C3	1.443	1.419	1.417	1.449	1.427	1.424	1.433
C3–C3	1.386	1.363	1.365	1.387	1.387	1.371	1.379
C3–C4	1.430	1.510	1.505	1.444	1.522	1.515	1.526
C4–C4	1.408	1.551	1.582	1.400	1.563	1.598	1.604
C4–X ^c		1.106	1.767		1.104	1.794	1.808

^a The length unit is Å. ^b The results of the last column are from ref 18. ^c X represents H or Cl.

Results and Discussion

1. Optimized Structures of Saturn-Shaped C₅₀Cl₁₀, C₅₀H₁₀, and C₅₀. First, we optimized the structures of *D*_{5h} C₅₀, Saturn-shaped C₅₀H₁₀, and C₅₀Cl₁₀, which are shown in Figure 1. There are four sets of nonequivalent C sites in *D*_{5h} C₅₀, which are denoted in Figure 1a. The 10 equatorial sites are type IV sites, which are PPH sites. They are believed to be the most active carbons in C₅₀; therefore 10 H or 10 Cl atoms are probably added to these locations.

The bond lengths of C₅₀ before and after addition are shown in Table 2. In C₅₀, there are six kinds of C–C bonds as listed in Table 2. Both GGA and LDA results are present in Table 2, and these two kinds of results are close to each other. We mainly discuss the GGA results. From Table 2, we see that in bare C₅₀, the longest bond is C1–C1 bond (1.450 Å) and the shortest one is C3–C3 (1.387 Å). They can be looked upon as single bond and double bond, respectively. These two lengths are very close to the single and double bond lengths in C₆₀, which are 1.44 and 1.39 Å, respectively,³⁰ or 1.45 and 1.40 Å, respectively.⁸ Similarly, C2–C3 can be viewed as a single bond. C1–C2 is close to being a double bond as well as the C4–C4 bond, while C3–C4 is close to a single bond. After passivation by ten H or ten Cl, the C3–C4 and C4–C4 bonds are lengthened significantly while the lengths of other C–C bonds are almost unaffected. The C4–C4 bond is longer in the Cl addition case than in the H addition case by 0.04 Å. This is probably because of the stronger Cl–Cl Coulomb repulsion than H–H repulsion. This repulsion pulls the two C atoms of the C4–C4 bond away from each other. The C–H bond length of C₅₀H₁₀ is 1.104 Å, which is equal to the C–H bond length 1.10 Å of C₆₀H₂.³⁰ The C–Cl bond length of C₅₀Cl₁₀ is 1.794 Å, which agrees well with the result 1.808 Å of ref 18. The calculated lengths of other bonds of C₅₀Cl₁₀ in our simulation also agree well with the results of ref 18, which can be seen clearly in Table 2. Table 2 also shows that in both C₅₀H₁₀ and C₅₀Cl₁₀, the C3–C3 bond is still the shortest one and the C1–C2 bond is the second shortest one. They are still double bonds, while C1–C1 and C2–C3 are still single bonds.

2. C₅₀H₁₁, C₅₀Cl₁₁, and C₅₀H₁₁: Site Activities. To investigate the energetic feature and reactivity of the single C sites in *D*_{5h} C₅₀ before and after passivation by 10 H atoms, we add only one atom (H or Cl) to C₅₀ and to Saturn-shaped C₅₀H₁₀. There are 4 isomers of C₅₀H₁₁ as well as C₅₀Cl₁₁ and 3 isomers of C₅₀H₁₁. The optimized structures of C₅₀H₁₁ isomers and their comparisons with C₅₀ are shown in Figure 2. The optimized structures of C₅₀H₁₁ isomers are shown in Figure 3.

It is easy to discern that C₅₀H₁₁, C₅₀Cl₁₁, and C₅₀H₁₁ all have open-shell electronic structures that will lead to open-shell doublet ground state. Therefore, it may be not very accurate to calculate the properties of these molecules using the spin-

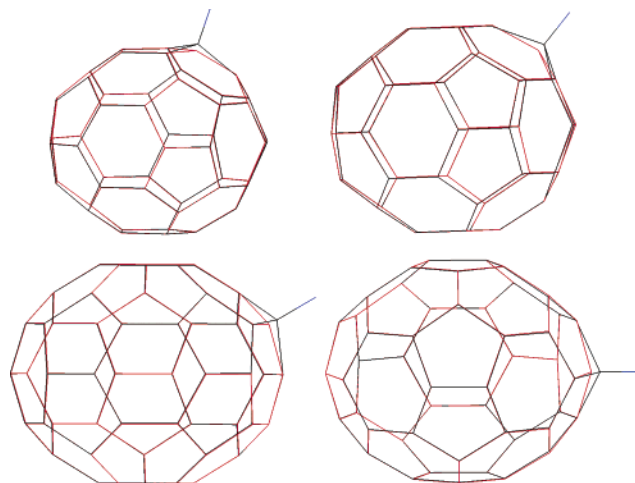


Figure 2. Schematic of four isomers of C₅₀H₁₁ (black and blue) and their comparisons with C₅₀ (red).

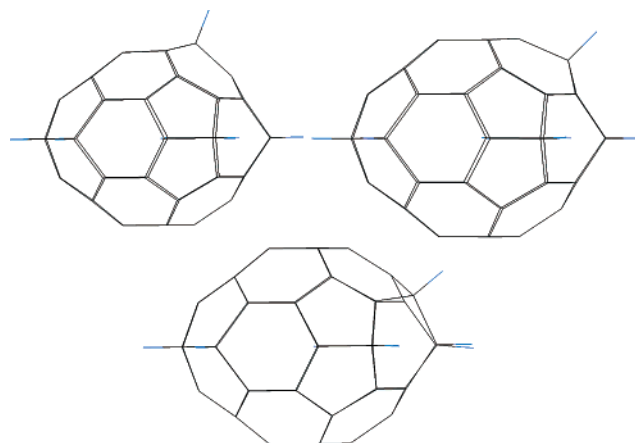


Figure 3. The three isomers of C₅₀H₁₁.

unpolarized DFT method adopted in this work. But from the previous theoretical works,^{6,8,32} we know that the energy of the open-shell ground state is close to that of the closed-shell state. For *D*_{6h} C₃₆, the energy difference between the two states is only 0.16 eV. Considering that the spin moment of the doublet state is only half of that of the triplet state, which is the ground state of C₃₆, the energy difference between the spin-unpolarized ground state and the spin-polarized ground state of C₅₀H₁₁, C₅₀Cl₁₁, or C₅₀H₁₁ is probably less than 0.1 eV. Therefore, it should be adequate to use the unpolarized DFT to semiquantitatively or qualitatively calculate the energetic properties of C₅₀H₁₁, C₅₀Cl₁₁, and C₅₀H₁₁.

Figure 2 shows that the C site linked to a H atom stretches outward notably, just as C₅₀H₁₀ and C₅₀Cl₁₀. This is easily understood when we take into account that the sp² bonding structure of that C is turned into sp³ bonding as it is passivated by H or Cl, and the sp³ bonding is nonplanar and tends to form pyramidal geometry. Figure 3 shows the similar feature of structural variations in C₅₀H₁₁. The binding energies of single H as well as single Cl added to four sites of C₅₀ were calculated and listed in Table 3. The binding energies of the 11th H of C₅₀H₁₁ isomers are listed in Table 4.

Table 3 shows that the binding energy of the C4 site is much higher than the other three. So H or Cl has larger probability to be adsorbed to site IV than to the others. This will be useful information in determining the favorable addition locations of *D*_{5h} C₅₀. In addition, Table 3 shows that the stability ordering of the 4 isomers is IV > II > III > I, which also can be viewed

TABLE 3: Binding Energies^a of Four Types of C Sites with One H or One Cl

C site	GGA				LDA			
	H E_B^b	E_{rel}^c	Cl E_B	E_{rel}	H E_B	E_{rel}	Cl E_B	E_{rel}
I	3.194	0.977	1.343	1.118	3.316	0.986	1.688	1.157
II	3.530	0.641	1.772	0.689	3.634	0.667	2.177	0.668
III	3.362	0.810	1.670	0.791	3.490	0.812	2.114	0.731
IV	4.171	0.000	2.461	0.000	4.302	0.000	2.845	0.000

^a The unit is eV. ^b E_B means binding energy. ^c E_{rel} means relative energy.

TABLE 4: Binding Energies of the 11th H of the Three Isomers of $C_{50}H_{11}$ and Their Relative Energies^a

C site	GGA		LDA	
	11th H E_B^b	E_{rel}^c	11 th H E_B	E_{rel}
I	2.766	0.103	2.866	0.101
II	2.406	0.463	2.506	0.461
III	2.869	0.000	2.966	0.000

^a All the energies are in eVs. ^b E_B means binding energy. ^c E_{rel} means relative energy.

as the activity ordering of the 4 sites of bare C_{50} . Table 3 also shows the parallel character of H and Cl additions. The stability order of the four $C_{50}H_1$ isomers is the same as that of $C_{50}Cl_1$ isomers; both are $IV > II > III > I$. Simultaneously, the relative energies of $C_{50}H_1$ isomers to the most stable one are very close to the corresponding ones of $C_{50}Cl_1$. The LDA computations give similar results.

Table 4 shows that the stability ordering of $C_{50}H_{11}$ isomers is $III > I > II$. Equivalently, this stability order is also the reactivity order of unsaturated C sites in Saturn-shaped $C_{50}H_{10}$. Such an order may give some suggestions for determining the preferential locations of further additions to Saturn-shaped $C_{50}H_{10}$. But this piece of experience should not be the sole rule to predict the favorite addition sites. In fact, there are other factors such as double-bond saturation³⁰ that may have greater impact on determining the favorable addition sites than binding energy ordering of single C sites.

3. $C_{50}H_{2m}$ ($m = 1\sim 7$) and Pseudo-Valency of D_{5h} C_{50} . To prove that the Saturn-shaped $C_{50}H_{10}$ as well as $C_{50}Cl_{10}$ is the pseudovalence structure of D_{5h} C_{50} , structural optimization and energetic and electronic structure calculations were carried out for $C_{50}H_{2m}$ ($m = 1\sim 7$) molecules. For each m , there are a lot of isomers, and it is almost impossible to simulate all the isomers to seek the most stable ones using the DFT method because of the prohibitively huge amount of computation. We carry out calculations on limited number of isomers as listed in Table 1. This is reasonable according to the conclusions in the preceding subsection on site activities and the reasons given in Computational Details. From the preceding subsection, we know that the equatorial C atoms are the most active for addition reaction. Furthermore, all equatorial sites of C_{50} are PPHs while all the others are PHHs. According to empirical rule, it is known that $PPH > PHH$ in reactivity. Consequently, we first add H atoms or H_2 molecules only to type IV sites until all C4 sites are passivated. Only in the cases of $m = 6$ and $m = 7$, two ($m = 6$) or four ($m = 7$) H atoms are added to non-IV sites. Therefore, the total number of isomers to be optimized is greatly reduced. The optimized structures of the most stable four isomers for each $C_{50}H_{2m}$ molecule are shown in Figure 4b–h. In each of these figures, the upper left one is the most stable one, the upper right is the second, the lower left is the third, and the lower right is the fourth. For each isomer, we computed the binding energies of H_2 molecules addition and the HOMO–LUMO gap.

These quantities for the best isomer of each m were extracted and the variations of them with m were analyzed.

3.1. Preferment of Site IV Addition and Experience for Determining the Favorable Addition Sites. It might be risky that only site IV addition isomers are taken into account to seek the most stable ones for $m = 1\sim 5$. To exclude the suspicion of the preferment of site IV additions, we did calculations on additional isomers of $C_{50}H_2$, $C_{50}H_8$, and $C_{50}H_{10}$ with one or two H atoms added to nonequatorial sites. The number of such isomers we took in our study is 40 for $C_{50}H_2$, 139 for $C_{50}H_8$, and 144 for $C_{50}H_{10}$. The constructions of these isomers are not random. For $C_{50}H_8$, when one H is added to a non-IV site, the other 7 H atoms are bound to neighboring C4 sites without a bare C4 site between them; when two Hs are added to non-IV sites, the addition pattern of the rest 6 Hs is just like that of the most stable isomer of $C_{50}H_6$ with only C4 addition. For $C_{50}H_{10}$, when one H is added to non-IV site, this H can be just taken from any C4 site of Saturn-shaped $C_{50}H_{10}$ because the ten Hs are all equivalent. When two Hs are added to non-IV sites, there are two schemes. In scheme (a), the two Hs are added to non-IV sites of the most stable isomer of $C_{50}H_8$ with only site IV addition. In scheme (b), the two Hs are added to non-IV sites of the second stable isomer of $C_{50}H_8$ with only C4 addition. The best two isomers of $C_{50}H_8$ with only C4 additions are shown in the upper part of Figure 4e. For $C_{50}H_2$, the constructions of additional isomers are random relative to $C_{50}H_8$ and $C_{50}H_{10}$, but the symmetry equivalent structures are excluded.

The relative energies and HOMO–LUMO gaps of the most stable five additional isomers for each of the three molecules are listed in Supporting Information, S-Table 1 in which the energies are relative to the corresponding best one of only C4 addition isomers. S-Table 1 shows that the energies of the additional isomers are much higher than that of the only site IV addition isomers, especially for $C_{50}H_2$ in which the best one of the additional isomers is even less stable than the worst one of only site IV addition isomers. For $C_{50}H_8$, the most stable one of non-IV addition isomers is less stable than the third stable one of only C4 addition isomers. Therefore, considering C4 sites as the preferred addition locations is reasonable and correct.

The most stable additional isomers for $C_{50}H_2$, $C_{50}H_8$, and $C_{50}H_{10}$ are shown in Supporting Information, S-Figure 1. From S-Figure 1, we can obtain some useful experience for predicting the favorable addition sites for further additions beyond $C_{50}H_{10}$.

S-Figure 1 shows that the best isomer of $C_{50}H_2$, $C_{50}H_8$, or $C_{50}H_{10}$ with non-IV additions is the one with only one H added to non-IV site, which further proves the preferment of site-IV addition. Double bond saturation is an important stabilizing factor as shown in S-Figure 1. The fifth stable additional isomer of $C_{50}H_2$, the second, third stable one of $C_{50}H_8$, and the second, third, fourth, and fifth one of $C_{50}H_{10}$ are all C3–C3 saturation cases. The fifth one of $C_{50}H_8$ is C1–C2 saturation case. All the first stable ones of the 3 molecules are actually C3–C4 saturation cases although the C3–C4 bond is closer to a single bond than to a double bond. In fact, in fullerenes there is no exact double bond or single bond as each bond is between double and single. In other words, each bond of fullerene contains more or less double-bond components. Usually it is believed that the shorter the C–C bond, the more double-bond component it has or the more unsaturated it is. S-Figure 1 also shows another stabilizing factor, the 1,4-addition of hexagon, which is also the favorite addition pattern in $C_{36}H_6$.^{6,10,13} The fourth stable one of $C_{50}H_2$ and the seventh stable one of $C_{50}H_8$

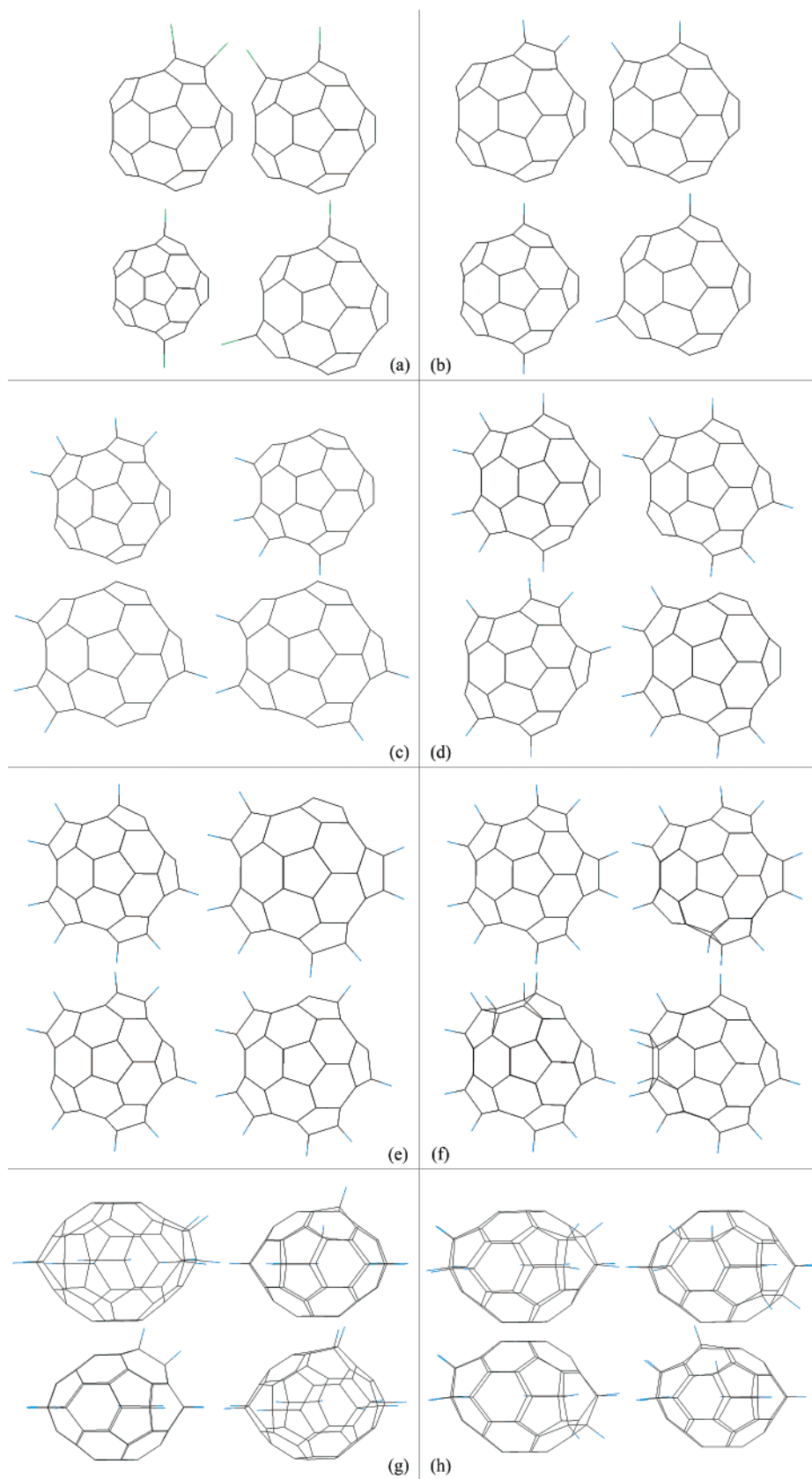


Figure 4. The most stable four isomers of $C_{50}Cl_2$ (a), $C_{50}H_2$ (b), $C_{50}H_4$ (c), $C_{50}H_6$ (d), $C_{50}H_8$ (e), $C_{50}H_{10}$ (f), $C_{50}H_{12}$ (g) and $C_{50}H_{14}$ (h). In each of the 8 insets, the upper left isomer is the most stable one, the upper right is the second stable one, the lower left is the third, while the lower right is the fourth.

are both this case. In fact, in Saturn-shaped $C_{50}H_{10}$ the saturation of ten C4 sites can be viewed as saturating five C4–C4 bonds and also can be viewed as 1,4-additions of 5 equatorial hexagons.

The experience for determining the favorable addition sites can be summarized into three points. First, binding energies of one-H additions give the activity order of nonequivalent sites. Second, double-bond saturation is a stabilizing factor, and the

shorter the (double) bond is, the greater stabilization of saturation it will lead to. Finally, 1,4-addition of hexagon is also a stabilizing factor. These experiences combined with the empirical rule about the site activity order, PPP > PPH > PHH > HHH, will greatly reduce the computation effort in search of the best isomers of C_nX_m .

3.2. *The Most Stable Isomers of $C_{50}H_{2m}$ with $m = 1\sim 7$.* Figure 4b–e shows the most stable isomers of $C_{50}H_{2m}$ for $m = 1, 2, 3$ and 4 with only C4 additions. Figure 4f shows the most stable 4 isomers of $C_{50}H_{10}$ with not only C4 addition. For only site IV addition cases, there are only 7 nonequivalent isomers for $m = 1$ or $m = 4$ and only 27 isomers for $m = 2$ or $m = 3$. All of them were optimized in our study to look for the best isomers. These figures show that at the equatorial belt the adsorbed H atoms tend to neighbor on each other without the bare C4 site between them. Actually, in the best isomer of $C_{50}H_{2m}$ ($m = 1\sim 5$), the addition to C4 sites can be viewed as saturating m C4–C4 bonds ($m = 1, 2, 5$), or 1,4-additions of m equatorial hexagons ($m = 3, 4, 5$). For $C_{50}H_8$, the stability order of all the 7 isomers agrees well with the results of ref 34.

The number of isomers we took in our work is 42 for $C_{50}H_{12}$ and 208 for $C_{50}H_{14}$. Ten H atoms have been preferably added to ten C4 sites, which greatly decreases the number of isomers to be considered. These isomers are chosen mainly according to the experience derived above, but there are still some isomers in which the addition sites are selected randomly. They are mainly used to further verify the preferred structures and to increase the reliability of the results. The best 4 isomers of $C_{50}H_{12}$ and $C_{50}H_{14}$ are shown in Figure 4g and Figure 4h, respectively.

In Figure 4g, double-bond saturation prevails among the isomers of $C_{50}H_{12}$. The most, third, and fourth stable one are all bond saturation configurations. In the best one, a C3–C3 bond is saturated, which is consistent with the above conclusions that C3 is the most active site in the Saturn-shaped $C_{50}H_{10}$, and that C3–C3 is the most unsaturated bond in $C_{50}H_{10}$. C1–C2 bond as the second reactive C–C bond of $C_{50}H_{10}$ is saturated in the third stable isomer. In the fourth stable one, C1–C1 bond is saturated. There is another double-bond saturation case, C2–C3 bond saturation, which is less stable than C1–C1 saturation by 0.407 eV and is the eighth stable one of the total 42 isomers in our study for $C_{50}H_{12}$. As a stabilizing pattern, 1,4-addition of hexagon also shows its importance in the second stable isomer of $C_{50}H_{12}$. Double-bond saturation continues to be favorable among the stable isomers of $C_{50}H_{14}$ as Figure 4h shows. Two C3–C3 bonds are saturated in all the most, second and third stable isomers, which further verifies the high activity of C3–C3 bond relative to other bonds in $C_{50}H_{10}$. In the fourth stable isomer of $C_{50}H_{14}$, a case of 1,4-addition of hexagon again occurs accompanied with a C3–C3 saturation, which further testifies the stabilization function of 1,4-addition of hexagon.

The calculated relative energies and HOMO–LUMO gaps of the best 4 isomers of $C_{50}H_{2m}$ for $m = 0\sim 7$ are listed in Table 5 in which the energy of the best isomer for each m is fixed at zero. Table 5 shows that in some cases ($m = 4, 5, 6$) the HOMO–LUMO gap of the most stable isomer is also the largest, but in other cases it is not. As the HOMO–LUMO gap is correlated to chemical stability,^{33,37} it should be pointed out that the most stable isomers mentioned above mainly mean that they are most stable physically or thermodynamically, but not necessarily most stable chemically. However, it can be convincing that the gap of the most stable isomer is also one of the largest several ones. Another obvious feature that can be seen in Table 5 is that energy gaps of all the best 4 isomers of each

TABLE 5: Relative Energies and Energy Gaps of the Most Stable Four Isomers of $C_{50}H_{2m}$

m	total energy (eV)				LUMO – HOMO (eV)			
	most	second	third	fourth	most	second	third	fourth
GGA								
0	0.000				0.468			
1	0.000	0.071	0.185	0.198	1.113	0.946	1.135	1.321
2	0.000	0.029	0.083	0.108	1.282	1.153	1.506	1.495
3	0.000	0.241	0.306	0.506	1.658	1.729	1.821	0.755
4	0.000	0.235	0.629	1.002	2.073	1.212	1.168	0.602
5	0.000	0.821	1.078	1.095	2.368	1.737	1.958	2.036
6	0.000	0.475	0.799	0.849	2.093	1.889	2.065	1.301
7	0.000	0.034	0.081	0.174	2.130	2.187	2.099	2.390
LDA								
0	0.000				0.230			
1	0.000	0.151	0.203	0.223	1.137	0.953	1.149	1.337
2	0.000	0.003	0.019	0.024	1.284	1.154	1.517	1.511
3	0.000	0.232	0.282	0.518	1.664	1.758	1.996	1.141
4	0.000	0.255	0.631	0.999	2.089	1.215	1.190	0.626
5	0.000	0.832	1.106	1.111	2.423	1.738	1.960	2.053
6	0.000	0.449	0.783	0.846	2.112	1.895	2.068	1.286
7	0.000	0.024	0.078	0.128	2.132	2.201	2.113	2.408

m are much larger than that of bare C_{50} , confirming the chemical stabilization function of hydrogenation. The LDA results also are given in Table 5 and are similar to GGA results.

3.3. *The Parallel Character of H_2 , Cl_2 Additions.* For comparison, the 7 isomers of $C_{50}Cl_2$ with only C4 additions also are optimized. The most stable 4 ones are shown in Figure 4a, which shows that they have the same addition patterns as the corresponding best $C_{50}H_2$ isomers shown in Figure 4b (i.e., $C_{50}Cl_2$ isomers and $C_{50}H_2$ isomers have identical stability orderings). Their relative energies, energy gaps, HOMOs, and LUMOs are listed in Table 6. The adding sites are denoted by two numbers that are the sequence numbers of the two C4 sites in clockwise direction. It can be seen that not only the energy order but also the energy gap order of 7 $C_{50}Cl_2$ isomers is the same as that of $C_{50}H_2$ ones. The relative energies of the isostructural isomers of the two molecules are close to each other. Most of the corresponding gap values are close to each other also. All these similarities further confirm that the hydrogenated and halogenated fullerenes have parallel energies and structures. The main difference is that both the LUMO and the HOMO levels of $C_{50}Cl_2$ isomers are deeper than that of isostructural isomers of $C_{50}H_2$, suggesting that $C_{50}Cl_2$ has larger ionization potential (IP) and electron affinity (EA) values than $C_{50}H_2$.^{33,35} The LDA results also are listed in Table 6 and give the similar conclusions.

3.4. *Energetic and Electronic Properties of the Most Stable Isomer of $C_{50}H_{2m}$ as Functions of m .* Figure 5 shows the energetic and electronic properties of the most stable isomer of $C_{50}H_{2m}$ as functions of m . Figure 5a shows the total binding energy of the best $C_{50}H_{2m}$ isomer as a function of m . Total binding energy is calculated as

$$E_b = E_{C_{50}} + mE_{H_2} - E_{C_{50}H_{2m}} \quad (1)$$

where $E_{C_{50}}$, E_{H_2} , and $E_{C_{50}H_{2m}}$ are the energies of C_{50} , H_2 , and $C_{50}H_{2m}$, respectively. This quantity also can be viewed as the reaction heat of the m H_2 molecules addition. Evidently, a kink or an inflection at $m = 5$ can be seen in Figure 5a. From $m = 1$ to $m = 5$, the GGA total binding energy almost linearly grows at 1.99 eV per added H_2 (2.29 for LDA). Beyond $m = 5$ ($2m = 10$), the curve is again approximately linear but with a smaller slope of 1.06 eV per H_2 (1.34 for LDA). Irrespective of systematic difference between the two methods (GGA and

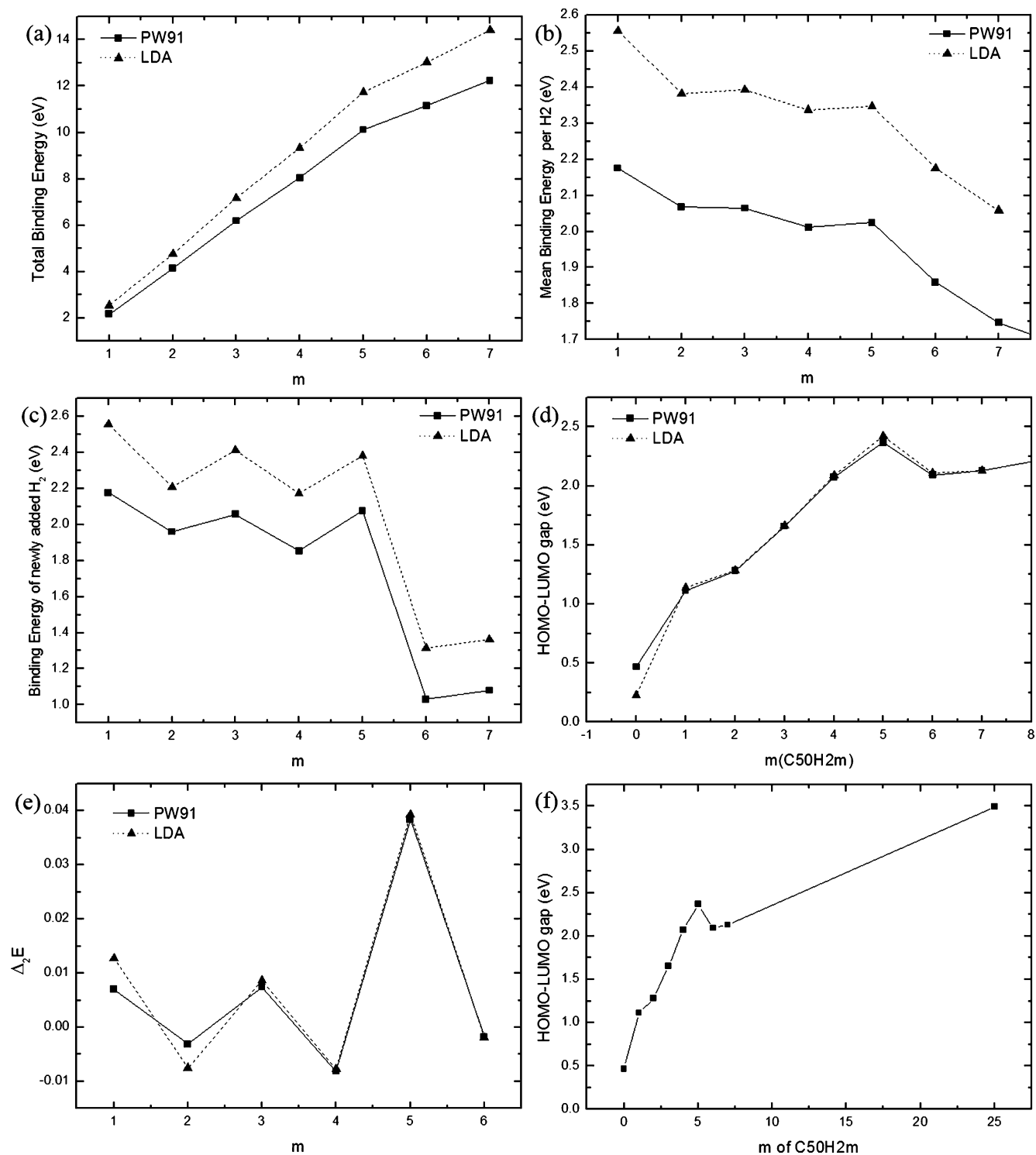


Figure 5. Energetic and electronic properties of the most stable isomer of $C_{50}H_{2m}$ as functions of m . (a) Total binding energy, (b) mean binding energy per H_2 molecule, (c) binding energy of newly added H_2 molecule, (d) energy gap, (e) the second order difference of energies, (f) energy gap variation trend in the whole range of m from 0 to 25, the part of $m \geq 8$ is only a qualitative description.

to C4 sites and if the two C4 sites are distant, the reaction barrier will be high. In C' , the two sites are neighboring while in C the two C4 sites are the most distant.

4. Valence Prediction of Other Fullerenes. In the above analyses, we have proved that 10 is the effective valence of D_{5h} C_{50} and that Saturn-shaped $C_{50}H_{10}$ as well as $C_{50}Cl_{10}$ is the magic-number stable adduct. But the interesting feature of HOMO–LUMO gap variation with m (the number of added H_2 molecules) and its relationship with the C site types (PPP, PPH, PHH, HHH) deserve more attention and discussion.

In our results, when adding one H_2 molecule to $C_{50}H_{10}$, the gap is decreased. Then with the further addition of one H_2 (to form $C_{50}H_{14}$), the gap begins to increase slowly. Then continuing to add H_2 molecules will probably make the gap continue to increase and exceed the gap of $C_{50}H_{10}$ at some value of m . Finally, when all C sites are occupied, the gap will get to a very large value, 3.49 eV, which is much larger than that of $C_{50}H_{10}$ (2.37 eV). This behavior of energy gap variation is similar to that of C_{60} addition. According to refs 30 and 37, the gap of C_{60} is 1.66 eV. When one H_2 is added to C_{60} to saturate

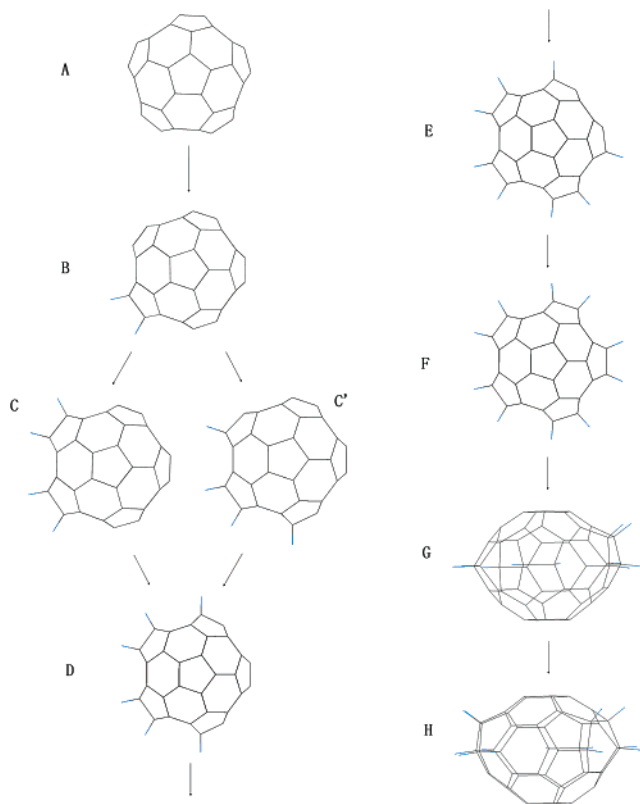


Figure 6. Minimal energy reaction pathway from C_{50} to $C_{50}H_{14}$.

a double bond, the gap is decreased to 1.45 eV; when two H_2 molecules are added to $C_{60}H_2$ to saturate another two double bonds and form a D_3 structure, the gap is increased to 1.63 eV. Finally, when all sites are hydrogenated, the gap reaches 3.64 eV. The similarity should be because the type of unsaturated C sites in Saturn-shaped $C_{50}H_{10}$ is identical to that in C_{60} and both are PHH type. In $C_{50}H_{10}$, ten PPH sites are saturated and all PHH sites are left. In $I_h C_{60}$, all sites are of PHH type. On the other hand, the peak value of HOMO–LUMO gaps for the best isomer series of $C_{50}H_{2m}$ is at $2m = 10$, which corresponds to the valence of $D_{5h} C_{50}$. That is, in the process of cumulative additions, when all PPH sites of C_{50} are saturated, the energy gap reaches local maximum and the chemical stability also becomes optimal. Taking into account that in classical fullerenes the site activity ordering is PPP > PPH > PHH > HHH,¹³ the singular point or local maximum of energy gap curve of $C_{50}H_{2m}$ actually occurs where all the more active sites of C_{50} , PPH sites, are hydrogenated or halogenated. This behavior is similar to the gap variation of the best $C_{24}H_{2m}$ series.¹¹ There are also two types of C sites in C_{24} . Twelve equatorial sites are of PPP type and others are of PPH type. When all PPP sites are hydrogenated, there is a significant jump on the gap curve. Then, another jump occurs when all PPH sites also are saturated.

According to the above discussion we infer that if there are two or more types of C sites in a classical fullerene and when the sites of a type with higher activity are all saturated, the HOMO–LUMO gap will undergo a sudden increase or reach a peak value, and thus a singular point will occur on the energy gap curve of C_nX_{2m} . At this moment, the number of added X atoms, $2m$, can be considered as a “valency” of the C_n cage “pseudoatom”. If further adding X_2 molecules beyond C_nX_{2m} , the gap will probably go on to increase slowly or first decrease then increase. But there will be no pronounced feature until all the sites of the second active type also are saturated by X atoms; then the new number of added atoms, $2m'$, will be another

valency of the superatom. We believe that this behavior of energy gap variation with m of C_nX_{2m} and its correlation with effective valences of fullerene should be general among classical fullerenes. This conclusion offers a simple method to determine the valences of smaller fullerenes and the optimal addition patterns of the C_n cages. Certainly, the additional “hidden” valences cannot be found by this simple steric method.

$D_3 C_{32}$ has been believed to be a divalent “superatom”.⁹ But according to our steric analysis, 26 also may be a valence of C_{32} . There are 3 types of sites in C_{32} : 2 PPP sites, 24 PPH sites, and 6 PHH sites. When 2 PPP sites are saturated, or 2 PPP sites plus 24 PPH sites are saturated, or all sites are saturated, on the HOMO–LUMO gap curve of $C_{32}H_{2m}$, a singular point will appear at $2m = 2$, $2m = 26$, or $2m = 32$. Therefore, 2, 26, and 32 are all probably the valences of $D_3 C_{32}$. Previous theoretical and experimental works have indicated that 6 is probably a valence of $D_{6h} C_{36}$.^{13,6,10} Our analysis indicates that there are 24 PPH sites and 12 PHH sites in this cage, and $C_{36}H_{24}$ with 24 H atoms added to the 24 PPH sites also should be a stable hydride. Accordingly, 24 may also be a valence of $D_{6h} C_{36}$. For $D_{5h} C_{50}$:1, there are 10 PPP sites, 10 PPH sites, 10 PHH sites, and 20 HHH sites. According to the steric method, we infer that 10, 20, and 30 are all the possible valences of this long superatom. In the above section, we have discussed the similarity of energy gap variation between further additions to $C_{50}H_{10}$ and additions to C_{60} . For fullerene C_n with $n > 60$, the IPR rule is satisfied. As each classical fullerene contains 12 pentagons, in IPR fullerenes there are a fixed number of PHH sites, which is $12 \times 5 = 60$. All the rest sites are HHH ones. We infer that when all the 60 PHH sites are saturated, a peak or a jump will probably also appear on the energy gap curve of C_nH_{2m} series. Therefore, it can be inferred reasonably that 60 is a common valence of IPR fullerenes.

Conclusions

In this paper, we report a computational investigation of C_{50} additions with H and Cl using DFT method. The energetic features and electronic properties of C_{50} adducts show the improved stability of Saturn-shaped $C_{50}H_{10}$ and $C_{50}Cl_{10}$ relative to $D_{5h} C_{50}$. $C_{50}H_1$, $C_{50}Cl_1$, $C_{50}H_{11}$, and $C_{50}H_{2m}$ ($m = 1\sim 7$) isomers are optimized to seek the most stable isomer of each molecule. The prime results obtained in this work are: (i) The binding energies and HOMO–LUMO gaps of these isomers clearly prove that Saturn-shaped $C_{50}H_{10}$ as well as $C_{50}Cl_{10}$ is a pseudo-valence structure of $D_{5h} C_{50}$ and $2m = 10$ is the effective valence of C_{50} fullerene. Thus, $C_{50}H_{10}$ as well as $C_{50}X_{10}$ may have the magic-number stability among molecules of $C_{50}X_{2m}$ series. (ii) A minimal energy reaction pathway is constructed to get $C_{50}H_{10}$ and $C_{50}H_{14}$. (iii) The preferment of C4-site addition is confirmed by single atom additions and by computations on additional isomers of $C_{50}H_2$, $C_{50}H_8$, and $C_{50}H_{10}$ with one or two H atoms added to nonequatorial sites. (iv) Some useful experience for determining the favorable addition sites was summarized, which will help to greatly decrease the computational effort in search of the best isomers of C_nX_m . (v) A simple steric method related to C-site types (PPP, PPH, PHH, and HHH) is developed to determine the effective valences of classical fullerenes, and the valences of some fullerenes are predicted using this method.

Acknowledgment. We thank Shanghai Supercomputing Centre for the use of the Dawning 4000A supercomputer. This work is partially supported by the Key Project of the Knowledge Innovation Programme of the Chinese Academy of Sciences (KJCX2-SW-N02).

Supporting Information Available: Relative energies and energy gaps of the best five additional isomers for $C_{50}H_2$, $C_{50}H_8$, and $C_{50}H_{10}$ with one or two H atoms added to non-C4 sites are listed in S-Table 1. The structures of the most stable additional isomers for $C_{50}H_2$, $C_{50}H_8$, and $C_{50}H_{10}$ are illustrated in S-Figure 1 and a part of the explanation and analysis is given following the figure. The optimized structure of $C_{50}H_{50}$ is shown in S-Figure 2. This material is available free of charge via the Internet at <http://pubs.acs.org>.

References and Notes

- (1) Kroto, H. W.; Heath, J. R.; O'Brien, S. S.; Curl, R. F.; Smalley, R. E. *Nature* **1985**, *318*, 162.
- (2) Kadish, K. M.; Ruoff, R. S., Eds. *Fullerene: Chemistry, Physics and Technology*; Wiley: New York, 2002.
- (3) Kroto, H. W. *Nature* **1987**, *329*, 529.
- (4) Albertazzi, E.; Domene, C.; Fowler, P. W.; Heine, T.; Seifert, G.; Alsenoy, C. V.; Zerbetto, F. *Phys. Chem. Chem. Phys.* **1999**, *1*, 2913.
- (5) Piskoti, C.; Yarger, J.; Zettl, A. *Nature* **1998**, *393*, 771.
- (6) Ito, A.; Monobe, T.; Yoshii, T.; Tanaka, K. *Chem. Phys. Lett.* **2000**, *328*, 32.
- (7) Jagadeesh, M. N.; Chandrasekhar, J. *Chem. Phys. Lett.* **1999**, *305*, 298.
- (8) Yuan, L.-F.; Yang, J.-L.; Deng, K.; Zhu, Q.-S. *J. Phys. Chem. A* **2000**, *104*, 6666.
- (9) Milani, C.; Giambelli, C.; Roman, H. E.; Alasia, F.; Benedek, G.; Broglia, R. A.; Sanguinetti, S.; Yabana, K. *Chem. Phys. Lett.* **1996**, *258*, 554.
- (10) Heine, T.; Fowler, P. W.; Rogers, K. M.; Seifert, G. *J. Chem. Soc., Perkin Trans. 2* **1999**, 707.
- (11) Fowler, P. W.; Heine, T.; Troisi, A. *Chem. Phys. Lett.* **1999**, *312*, 77.
- (12) Fowler, P. W.; Heine, T.; Rogers, K. M.; Sandall, J. P. B.; Seifert, G.; Zerbetto, F. *Chem. Phys. Lett.* **1999**, *300*, 369.
- (13) Fowler, P. W.; Heine, T. *J. Chem. Soc., Perkin Trans. 2* **2001**, 487.
- (14) Heine, T.; Fowler, P. W.; Seifert, G. *Solid State Commun.* **1999**, *111*, 19.
- (15) Menon, M.; Richter, E. *Phys. Rev. B* **1999**, *60*, 13322.
- (16) Huang, Y.; Chen, Y.; Liu, R. *J. Phys. Chem. Solids* **2000**, *61*, 1475.
- (17) Grossman, J. C.; Louie, S. G.; Cohen, M. L. *Phys. Rev. B* **1999**, *60*, R6941.
- (18) Xie, S.-Y.; Gao, F.; Lu, X.; Huang, R.-B.; Wang, C.-R.; Zhang, X.; Liu, M.-L.; Deng, S.-L.; Zheng, L.-S. *Science* **2004**, *304*, 699.
- (19) Kroto, H. W.; Walton, D. R. M. *Chem. Phys. Lett.* **1993**, *214*, 353.
- (20) Hohenberg, P.; Kohn, W. *Phys. Rev.* **1964**, *136*, 864.
- (21) Bockstedte, M.; Kley, A.; Neugebauer, J.; Scheffler, M. *Comput. Phys. Commun.* **1997**, *107*, 187.
- (22) Kohn, W.; Sham, L. J. *Phys. Rev.* **1965**, *140*, 1133.
- (23) Ihm, J.; Zunger, A.; Cohen, M. L. *J. Phys. C* **1979**, *12*, 4409.
- (24) Fuchs, M.; Scheffler, M. *Comput. Phys. Commun.* **1999**, *119*, 67.
- (25) Hamann, D. R. *Phys. Rev. B* **1989**, *40*, 2980.
- (26) Kleinman, L.; Bylander, D. M. *Phys. Rev. Lett.* **1982**, *48*, 1425.
- (27) Wang, Y.; Perdew, J. P. *Phys. Rev. B* **1991**, *44*, 13298.
- (28) Ceperley, D. M.; Alder, B. J. *Phys. Rev. Lett.* **1980**, *45*, 567.
- (29) Perdew, J. P.; Zunger, A. *Phys. Rev. B* **1981**, *23*, 5048.
- (30) Yi, J.-Y.; Bernholc, J. *Chem. Phys. Lett.* **2005**, *403*, 359.
- (31) Fuchs, M.; Penev, E. *Tutorial of FHI98PP*; 2003. Available online at <http://www.fhi-berlin.mpg.de/th/fhi98md/fhi98PP/tutorial.ps>.
- (32) Ito, A.; Monobe, T.; Yoshii, T.; Tanaka, K. *Chem. Phys. Lett.* **1999**, *315*, 348.
- (33) Kietzmann, H.; Rochow, R.; Gantefor, G.; Eberhardt, W. *Phys. Rev. Lett.* **1998**, *81*, 5378.
- (34) Zhechkov, L.; Heine, T.; Seifert, G. *J. Phys. Chem. A* **2004**, *108*, 11733.
- (35) Lu, X.; Chen, Z. F.; Thiel, W.; Schleyer, P. R.; Huang, R. B.; Zheng, L. S. *J. Am. Chem. Soc.* **2004**, *126*, 14871.
- (36) Zhao, X. *J. Phys. Chem. B* **2005**, *109*, 5267.
- (37) Wu, H.-P.; Deng, K.-M.; Yang, J.-L.; Wang, X. A study on Structural and Electronic Property of $C_{60}H_6$; 2003. Available online at <http://edu.qiji.cn/eprint/abs/325.html>.
- (38) Chen, Z. F. *Angew. Chem., Int. Ed.* **2004**, *43*, 4690.
- (39) Xie, R.-H.; Bryant, G. W.; Cheung, C. F.; Smith, V. H., Jr.; Zhao, J. *J. Chem. Phys.* **2004**, *121*, 2849.